SP2509, a Selective Inhibitor of LSD1, Suppresses Retinoblastoma Growth by Downregulating β-catenin Signaling

Alan Jiang,[1] Weiqi Wu,[2,3] Caixia Xu,[2,3] Longbing Mao,[2,3] Sha Ao,[2,3] Huifeng Guo,[2,3] Xiantao Sun,[4] Jing Tao,[4] Yi Sang,[1] and Guofu Huang[1,2]

[1]Jiangxi Provincial Key Laboratory of Tumor Metastasis and Precision Therapy, Center Laboratory, The Third Affiliated Hospital of Nanchang University, Nanchang, Jiangxi, PR China
[2]Department of Ophthalmology, The Third Affiliated Hospital of Nanchang University, Nanchang, Jiangxi, PR China
[3]Medical Department of Graduate School, Nanchang University, Nanchang, Jiangxi, PR China
[4]Department of Ophthalmology, Children's Hospital Affiliated to Zhengzhou University, Henan Children's Hospital, Zhengzhou Children's Hospital, Zhengzhou, Henan, PR China

Correspondence: Guofu Huang, Jiangxi Provincial Key Laboratory of Tumor Metastasis and Precision Therapy, Center Laboratory, The Third Affiliated Hospital of Nanchang University, 128 Xiangshan Northern Road, Nanchang, Jiangxi 330008, PR China; hgf2222@sina.com.

AJ and WW contributed equally to this work.

Received: June 28, 2021
Accepted: November 11, 2021
Published: March 17, 2022

Citation: Jiang A, Wu W, Xu C, et al. SP2509, a selective inhibitor of LSD1, suppresses retinoblastoma growth by downregulating β-catenin signaling. *Invest Ophthalmol Vis Sci.* 2022;63(3):20. https://doi.org/10.1167/iovs.63.3.20

Purpose. To study the role of lysine-specific demethylase 1 (LSD1) in retinoblastoma (RB) growth and to determine whether the LSD1 inhibitor SP2509 can inhibit RB progression.

Methods. We detected the levels of LSD1 in 12 RB tissue samples, two RB cell lines (Y79 and Weri-RB1), and a retinal pigment epithelium cell line (ARPE-19). Overexpression or knockdown of LSD1 was performed to examine the role of LSD1 in RB cancer cell survival. In vitro and in vivo experiments were conducted to detect the antitumor effect of SP2509, and the antitumor mechanism of SP2509 was examined by RNA sequencing and Western blot.

Results. LSD1 is overexpressed in RB tissues and cells and increases RB cancer cell viability and colony formation ability. The LSD1 inhibitor SP2509 inhibits RB cell proliferation in vitro and in vivo. Treatment with SP2509 increases the levels of dimethylated histone 3 lysine 4 (H3K4me2) and inhibits the expression of β-catenin signaling pathway–related proteins in RB cells.

Conclusions. We demonstrated that LSD1 is overexpressed in RB cells and promotes RB cell survival. The LSD1 inhibitor SP2509 exerted strong growth inhibition in vitro and in vivo, which was at least partially mediated by suppression of the β-catenin pathway.

Keywords: retinoblastoma (Rb), LSD1, SP2509, β-catenin

Retinoblastoma (RB) is a rare, aggressive childhood cancer, with a global incidence of 1:15,000 to 1:20,000 cases annually.[1] Despite improvements in therapy with local intravitreal or intra-arterial chemotherapy and a 5-year survival rate of 97%, drug toxicity remains a major obstacle in treating RB, especially with respect to the increased risk of secondary malignant neoplasms.[2–4] Thus, new therapeutic options need to be explored.

Lysine-specific demethylase 1 (LSD1), also known as KDM1A, demethylates mono- and dimethylated Lys4 and Lys9 of histone 3 (H3K4 and H3K9) to mediate target gene transcription.[5,6] LSD1 is a component of multiple large repressive complexes, including cofactor of RE1-silencing transcription factor and nucleosome remodeling and histone deacetylase, that coordinate histone acetylation and methylation to control target gene transcription.[7] LSD1, which is highly expressed in several solid and hematologic cancers, is directly correlated with worse prognosis, and LSD1 inhibition significantly reduces tumor growth.[8–12] Numerous preclinical statistical studies have confirmed that LSD1 can selectively inhibit acute myeloid leukemia (AML) and solid tumors, which has bolstered the subsequent clinical application value of LSD1 antagonists for these diseases.[8,13]

SP2509, a selective LSD1 antagonist, exerts significant antitumor activity in a variety of cancers.[14] In AML, SP2509 and the pan–histone deacetylase (HDAC) inhibitor panobinostat exerted synergistic lethality against AML blasts. A study of clear cell renal cell carcinoma by Jin Zhang et al.[15] revealed that SP2509 observably suppressed cell proliferation, induced G1/S phase arrest, and mitigated renal xenograft tumor growth. LSD1 has elevated expression in and is a therapeutic target for Ewing sarcoma.[16] However, the role of LSD1 in RB and the mechanism responsible for its therapeutic effect remain largely unknown.

In this study, we explored the role of LSD1 in the progression of RB and demonstrated that the LSD1 inhibitor SP2509 partially blocked RB cell survival via suppression of β-catenin signaling.

Table 1. Clinical Features of Patients With RB

Characteristic	Number
Sex	
Male	5
Female	7
Laterality	
OD	5
OS	7
Age, y	
<3	7
≥3	5
Stage	
II	2
IIN	1
III	3
IV	6

OD, OculusDexter, right eye; OS, OculusSinister, left eye.

Materials and Methods

Study Approval and Patient Samples

Experiments involving human RB tissues were approved by the Ethical Committee of The Third Affiliated Hospital of Nanchang University (KY2021057). All human samples were obtained from 12 patients with RB who underwent surgery at the eye hospital of Wenzhou Medical University and Zhengzhou Children's Hospital. The clinical information of the patients is summarized in Table 1.

Hematoxylin and Eosin Staining and Immunohistochemistry

To examine the structure and LSD1 protein level, hematoxylin and eosin staining and immunohistochemistry (IHC) were performed as described in our previous study.[17] For IHC, paraffin sections were heated at 60°C for 2 hours, deparaffinized with xylene, and rehydrated with a graded alcohol series. After they were boiled in Tris-EDTA for antigen retrieval and treated with a 3% H_2O_2 solution to block endogenous peroxidase activity, the sections were incubated in the primary antibody against LSD1 (1:800, cat. 2184; Cell Signaling Technology, Danvers, MA, USA) at 4°C overnight. The next day, the washed sections were incubated in horseradish peroxidase–conjugated goat anti-rabbit IgG (KIT-5010; Maixin, Fuzhou, China) at 37°C for 30 minutes. The immunostaining signals were visualized by diaminobenzidine (DAB), and sections were counterstained with hematoxylin; two pathologists examined the stained sections. The score for the percentage of positively stained cells was determined as follows: 0 (negative), 1 (<25%), 2 (26%–50%), 3 (51%–75%), and 4 (>75%); the staining intensity score for LSD1 was defined as follows: 0 (negative), 1 (weak), 2 (moderate), and 3 (strong). The final immunoreactivity score was calculated by multiplying the percentage of the stained cells score and the intensity score.

Cell Culture and Reagents

Y79, Weri-RB1, ARPE-19, and 293T cells were purchased from the Institute of Biochemistry and Cell Biology (Shanghai, China). Weri-RB1 cells were cultured in RPMI 1640 medium (Gibco, Thermo Fisher Scientific, Waltham, MA, USA) containing 10% fetal bovine serum (FBS) (Gibco, Thermo Fisher Scientific, Waltham, MA, USA) and 1% penicillin-streptomycin in a 37°C humidified incubator with 5% CO_2. Y79, 293T, and ARPE-19 cells were cultured at 37°C in Dulbecco's modified Eagle's medium (DMEM) (Gibco, Thermo Fisher Scientific, Waltham, MA, USA) containing 10% FBS and 1% penicillin-streptomycin. SP2509 was purchased from Selleck (Houston, TX, USA), and stock solutions were diluted in DMSO at an initial concentration of 10 mM.

Lentivirus Acquisition and Stable Cell Line Construction

The lentivirus packaging vectors used were packaging plasmid psPAX2 and envelope plasmid pMD2.G. HA-puro vector containing the LSD1 coding region or empty vector was cotransfected with the packaging vectors into HEK-293T cells at a suitable ratio with the transfection reagent Lipofectamine 2000 (Invitrogen, Thermo Fisher Scientific, Carlsbad, MA, USA). After 48 hours, the supernatants were subsequently collected and filtered through a 0.45-µm filter (Millipore, Temecula, CA, USA), and then concentrated virus with 8 µg/mL polybrene was used to infect Y79 cells for 24 hours. Stably infected cells were selected with 0.5 µg/mL puromycin for 2 weeks, and the cells were collected and subjected to Western blot used to detect the protein level of LSD1.

Electroporation

For electroporation assays, Weri-RB1 cells (2×10^6 cells/well) were suspended in 200 µL Cytomix electroporation buffer (90% RPMI-1640 + 10% DMSO) with 8 µL targeted small interfering RNA (siRNA) or negative control (NC) siRNA (160 µM). The sequences were as follows: siLSD1#1, 5′-CUACAUCUUACCUUAGUCATT-3′ (sense), 5′-UGACUAAGGUAAGAUGUAGTT-3′ (antisense); siLSD1#2, 5′-CAGCUGACAUUUGAGGCUATT-3′ (sense), 5′-UAGCCUCAAAUGUCAGCUGTT-3′ (antisense). The suspensions were transferred into 0.2-cm precooled electroporation cuvettes, incubated on ice for 30 minutes, and electroporated at 0.15 kV/975 µF/∞. Electroporation was carried out using a high-voltage pulser (GenePulser Xcell; Bio-Rad, CA, USA), after which cells were seeded in 6-well plates, cultured for 48 hours, and then subjected to Western blot to detect the protein level of LSD1.

Viability Assay

The viability of Y79 and Weri-RB1 cells was detected by an methylthiazolyldiphenyl-tetrazolium bromide (MTT) assay as described previously.[17] Briefly, cells were seeded in 96-well plates (5000 cells/well) in the presence or absence of a series of compounds at different concentrations for 24, 48, 72, and 96 hours. Then, 20 µL MTT (cat. C0009S, 5 mg/mL; Beyotime, Biotechnology, Beijing, China) was added to each well, and the plates were incubated for another 4 hours in the dark. Finally, the formazan crystals were dissolved in DMSO, and cell viability was assessed by evaluating the optical density of each well at 490 nm. Cell viability inhibition was calculated using GraphPad Prism software (version 8.0; GraphPad Software, La Jolla, CA, USA), and all experiments were repeated three times.

RNA Extraction and Real-Time Polymerase Chain Reaction

Total RNA was extracted using TRIzol reagent (Invitrogen, Carlsbad, CA, USA), and complementary DNA was obtained

Investigative Ophthalmology & Visual Science

Table 2. Primer Sequences Used for RT-PCR Analysis in Our Study

Gene	Forward Primer (5′ → 3′)	Reverse Primer (5′ → 3′)
GAPDH	GGAGCGAGATCCCTCCAAAAT	GGCTGTTGTCATACTTCTCATGG
LSD1	TGACCGGATGACTTCTCAAGA	GTTGGAGAGTAGCCTCAAATGTC
P16	GATCCAGGTGGGTAGAAGGTC	CCCCTGCAAACTTCGTCCT
P19	AGTCCAGTCCATGACGCAG	ATCAGGCACGTTGACATCAGC
P21	TGTCCGTCAGAACCCATGC	AAAGTCGAAGTTCCATCGCTC
GADD45β	TGCTGTGACAACGACATCAAC	GTGAGGGTTCGTGACCAGG
MYC	GGCTCCTGGCAAAAGGTCA	CTGCGTAGTTGTGCTGATGT
Cyclin D3	TACCCGCCATCCATGATCG	AGGCAGTCCACTTCAGTGC

using the PrimeScript RT reagent kit (TaKaRa, Beijing, China) according to the manufacturer's protocol. The primer sequences used in our study are shown in Table 2. All real-time quantitative polymerase chain reaction (RT-PCR) was performed with SYBR Green reagents on a CFX96 Real-Time System (Bio-Rad, CFX96 optics module). Expression levels were calculated relative to the level of the control gene using the $2^{-\Delta\Delta CT}$ method.

Western Blot Assay

Cells were harvested and lysed in RIPA buffer (150 mM NaCl, 50 mM Tris Base, 50 mM EDTA, 1% NP40) supplemented with protease inhibitor. Protein quantification was performed using the Coomassie brilliant blue G-250 method. Proteins were separated by sodium dodecyl sulfate–polyacrylamide gel electrophoresis through 8% to 10% gels and transferred to 0.45-µm polyvinylidene fluoride membranes (Millipore Corp., Bedford, MA, USA), which were incubated with 5% skim milk for 1 hour to block nonspecific binding sites. The membranes were then incubated overnight at 4°C with the following primary antibodies: anti-LSD1 (1:1000, Cell Signaling Technology, Danvers, MA, USA, cat. 2184), anti–β-catenin (1:1000, ProteinTech, Rosemont, IL, USA, cat. 51067-2-AP), anti-H3K4me2 (1:1000, Cell Signaling Technology, Danvers, MA, USA, cat. 9725), anti–β-actin (1:1000, Servicebio, cat. GB12001), anti–c-MYC (1:1000, ProteinTech, cat. 10828-1-AP), anti–cyclin D3 (1:1000, Cell Signaling Technology, Danvers, MA, USA, cat. 2936), anti–caspase 3 (1:1000, Cell Signaling Technology, Danvers, MA, USA, cat. 14220T), anti–cleaved caspase 3 (1:1000, Cell Signaling Technology, Danvers, MA, USA, cat. 9664T), and anti-poly(ADP-ribose)polymerase (PARP) (1:1000, Cell Signaling Technology, Danvers, MA, USA, cat. 9532). The membranes were washed three times in PBST (PBS containing 0.1% Tween) and incubated with the appropriate secondary antibody (anti-mouse IgG, 1:15,000, Promega, Madison, WI, USA, cat. W4021 or anti-rabbit IgG, 1:15,000, Promega, cat. W4011) at room temperature for 1 hour before the protein bands were visualized with chemiluminescence (Thermo Scientific, Waltham, MA, USA).

Cell Cycle Assay

Flow cytometry was used to evaluate the influence of compounds on the cell cycle. Briefly, cells (10×10^5 cells/well) were plated in triplicate in a 12-well plate, incubated for 48 hours, collected, washed two times with PBS, and fixed with precooled 70% ethanol for 2 hours at 4°C or −20°C overnight. Subsequently, the fixed cells were centrifuged at 1500 rpm for 5 minutes and washed twice with PBS again before they were incubated with 300 µL of staining solution buffer containing 50 µg/mL propidium iodide (PI) and 100 µg/mL RNase A for 15 minutes at room temperature in the dark. The results were analyzed using FlowJo 7.6 software (BD FACSCalibur; BD, NJ, USA).

Colony Formation Assay

A soft agar assay was used to analyze Y79 and Weri-RB1 cell colony formation. Before the experiment, high-pressure, steam-sterilized 1.2%, 0.6% agarose (cat. 2276GR005; BioFroxx, Germany) and 2× medium (RPMI 1640 with 40% FBS, 2% P/S, DMEM with 40% FBS, and 2% Penicillin-Streptomycin (P/S)) were prepared and cooled to 45°C. Agar for coating the plate wells was made as follows: 1.2% soft agarose with medium was mixed at a 1:1 ratio, and 500 µL was added per well of a 24-well plate and cooled at room temperature for 30 minutes. For the upper agar layer, cells were counted with a Cellometer Auto T4 (Nexcelom, Lawrence, MA, USA) and diluted with 2× medium. Then, medium containing 10^3–2×10^3 cells was mixed with the same volume of 0.6% soft agarose and plated on top of the agar layer coating the plate wells. After cells were cultured for at least 2 weeks, the morphology of the colonies was analyzed using cell staining, and the number of colonies formed per well was quantified using ImageJ (National Institutes of Health, Bethesda, MD, USA) software. ARPE-19 cells were plated into 24-well plates and cultured in DMEM containing a concentration series of SP2509. After 10 days, cells were stained with 0.2% crystal violet for 30 minutes, and then the colonies were photographed and counted.

Apoptosis Analysis Using Flow Cytometry

Apoptosis was evaluated using an Annexin V fluorescein (FITC)/PI double-staining cell apoptosis detection kit (KeyGen Biotech, Nanjing, China, cat. KGA107). Briefly, the cells were collected, washed twice with PBS, and then resuspended in 300 µL binding buffer containing 3 µL Annexin V FITC and 3 µL PI; the suspensions were incubated for 15 minutes at room temperature. The samples were analyzed using FlowJo software (BD FACSCalibur). FITC-positive events represent apoptotic cells, and the apoptosis ratio was calculated as the sum of the percentage of events in the Q2 and Q3 regions. All experiments were repeated three times.

RNA Sequencing Analysis

Y79 cells treated with 5 µM SP2509 for 48 hours showed the greatest inhibition of cell growth, so we chose a concentration of 5 µM for subsequent experiments. Three biological replicates of Y79 cells treated with 5 µM SP2509 or DMSO for 48 hours were prepared. The cells were washed three times, and the supernatants were removed and frozen in liquid nitrogen before they were sent to the Beijing Genomics

Investigative Ophthalmology & Visual Science

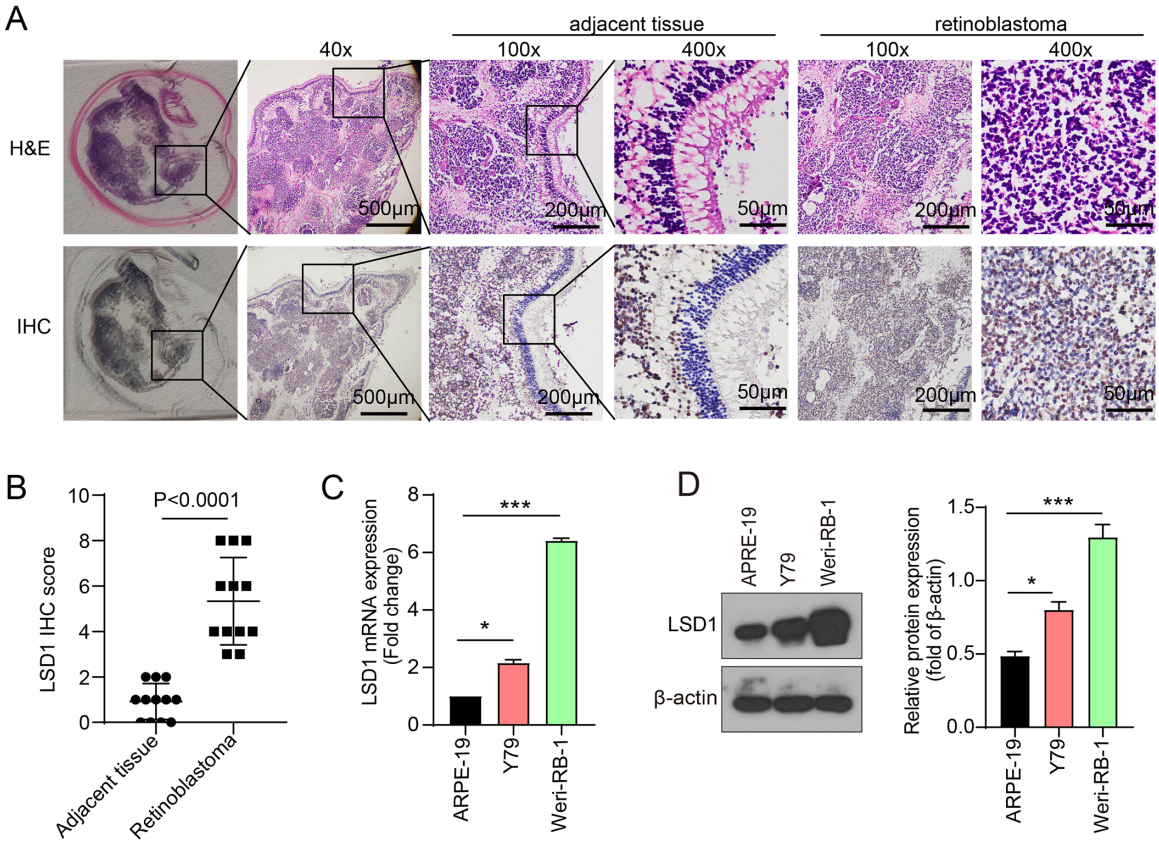

Figure 1. LSD1 is overexpressed in RB tissues and cells. (**A**, **B**) Hematoxylin and eosin and IHC staining (**A**) and statistical analysis (**B**) of LSD1 expression in human RB tissues and adjacent healthy tissues ($n = 12$). Student's t-test, $P < 0.0001$. *Scale bars*: 500 μm, 200 μm, and 50 μm, respectively. (**C**, **D**) Quantitative PCR (**C**) and Western blot assays (**D**) indicated that the messenger RNA (mRNA) and protein levels, respectively, of LSD1 in RB cells were higher than those in normal cells. The data are reported as the means ± standard deviations ($n = 3$), Student's t-test, $^{*}P < 0.05$, $^{***}P < 0.001$.

Institute (BGI) on dry ice to construct a sequencing library using the BGISEQ-500 platform. In this study, the BGI bioinformatics service system was used to confirm the significance of differentially expressed genes (absolute value of $\log_2$-ratio ≥ 1 and $P \leq 0.05$). The differentially expressed genes related to cellular biogenic activities were identified using heatmaps and Kyoto Encyclopedia of Genes and Genomes (KEGG) pathway analyses.

Xenotransplantation Experiments

For most subcutaneous xenograft experiments involving retinoblastoma, Y79 cells are usually injected subcutaneously into nude mice because these cells have stronger tumorigenicity and a higher cell growth rate[18,19]; therefore, we established a Y79 cell xenograft model in nude mice for in vivo evaluation. All animal experiments were performed according to protocols approved by Nanchang University (KY2021057). Fourteen male BALB/C nude mice (18–20 g, 4–5 weeks old) were obtained from Hunan SJA Laboratory Animal Co., Ltd. (Hunan, China) and housed in sterile conditions at a temperature of 20°C to 25°C and 50% to 70% humidity under a light/dark cycle of 12 hours with free access to water and food. A total of 1×10^7 cells in 0.2 mL PBS (pH 7.4) and 30% (v/v) Matrigel matrix (Corning Inc., Corning, NY, USA) were injected into the right submaxillary region of the mice. Two weeks later, we evaluated the tumor-bearing status of the mice and divided them into two groups: the SP2509-treated group (intraperitoneal injection of SP2509 [25 mg/kg, once a day]) and control group (intraperitoneal injection of an equal volume of vehicle [0.1% DMSO]); mice continued treatment for 3 weeks. The tumor volume and total body weights of the mice were measured twice a week. The tumor size was calculated according to the following formula: tumor volume (mm^3) = $(a \times b^2)/2$, where a is the length and b is the width of the tumor.

Statistical Analysis

All data are reported as the means ± standard deviations as indicated in the figure legends, and the statistical significance of differences between two groups was determined using the two-tailed Student's t-test. All cell culture experiments were performed at least three times independently. P values <0.05 were considered statistically significant.

Results

LSD1 Expression Is Increased in RB Tissues and Cells

Prior reports have demonstrated that LSD1 is an ideal therapeutic target for a variety of cancers, such as AML[8] and small cell lung carcinoma[20] owing to its high expression. Nevertheless, the underlying role of LSD1 in RB is unclear. Therefore, we examined the levels of LSD1 in RB tissue samples and RB cell lines (Y79, Weri-RB1). The IHC results showed that LSD1 expression was significantly higher in RB tissues

Investigative Ophthalmology & Visual Science

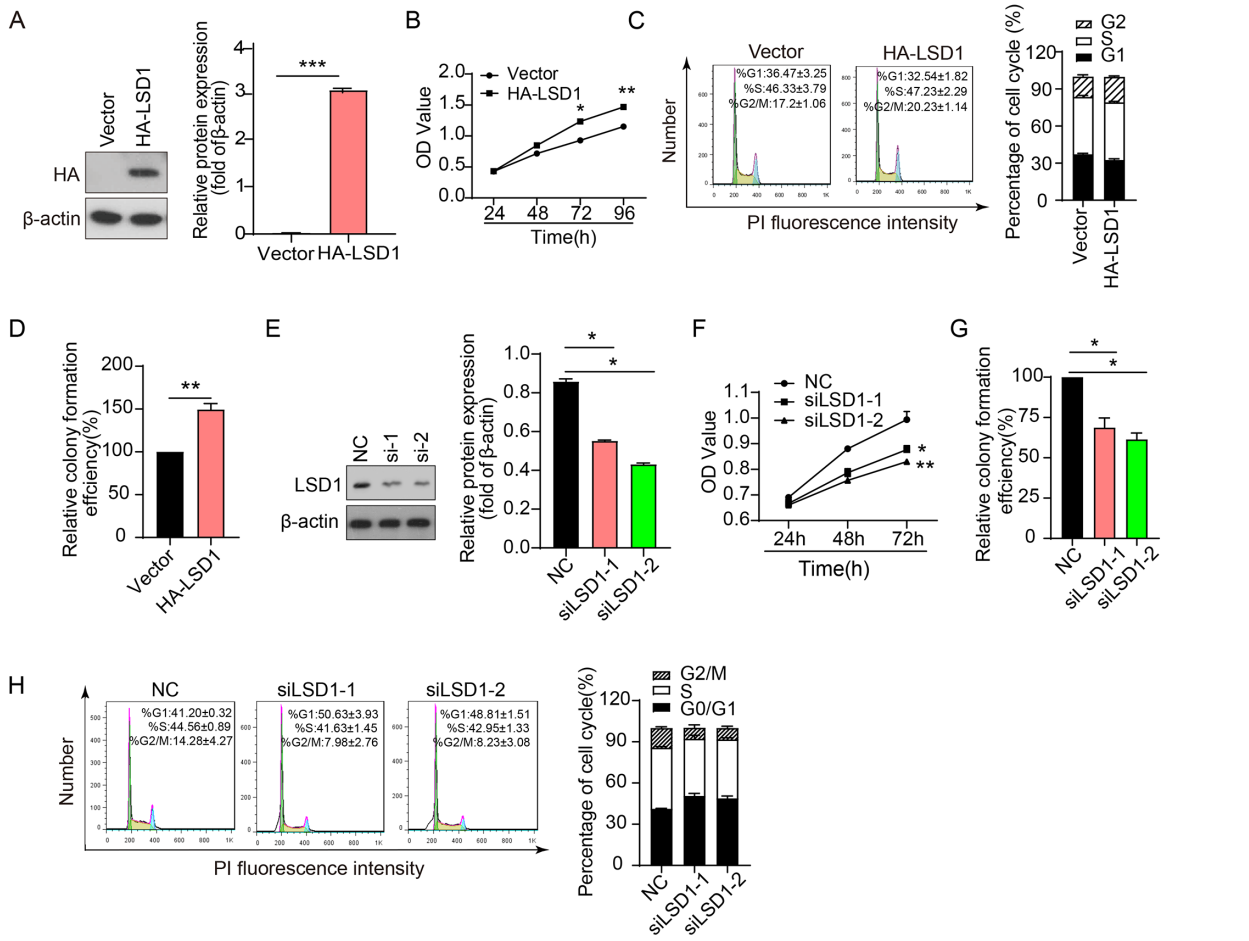

Figure 2. LSD1 overexpression promotes tumor growth, and knockdown of LSD1 suppresses cell proliferation in RB. (**A**) Y79 cells stably overexpressing LSD1. (**B**) The MTT assay showing proliferation of cells overexpressing LSD1. The data are reported as the means ± standard deviations ($n = 3$). Student's t-test, $^*P < 0.05$, $^{**}P < 0.01$, (**C**) Colony formation assay showed the colony-forming ability of the indicated cells. (**D**) Knockdown of LSD1 in Weri-RB1 cells by siRNA. (**E**, **F**) Cell viability and number of colonies produced in cells with LSD1 knockdown. The data are reported as the means ± standard deviations ($n = 3$), Student's t-test, $^*P < 0.05$, $^{**}P < 0.01$, $^{***}P < 0.001$.

than that in adjacent tissues (Figs. 1A, B). In addition, the messenger RNA and protein levels of LSD1 were significantly increased in RB cells compared with the negative control retinal pigment epithelium cell line (ARPE-19) (Figs. 1C, D). These data show that LSD1 was overexpressed in RB tissues and cells.

LSD1 Overexpression Promotes Tumor Survival, and Knockdown of LSD1 Suppresses Cell Proliferation in RB

The influence of LSD1 on RB cell proliferation was subsequently investigated. Stable Y79 cells with LSD1 overexpression were constructed (Fig. 2A) and used to assess the ability to promote cell survival. The results of the MTT and colony formation assays showed that high LSD1 expression was favorable for cell proliferation (Figs. 2B, D). Overexpression of LSD1 weakly promoted cells from G1 phase to S/G2 phase (Fig. 2C). To investigate the impact of downregulating LSD1 expression on cell proliferation, we transferred two small interfering fragments (siLSD1-1, siLSD1-2) or NC siRNA into Weri-RB1 cells via electroporation (Fig. 2E). MTT and colony formation assays demonstrated that downregulation of LSD1 inhibited RB cell proliferation (Figs. 2F, G). Downregulation of LSD1 induced cell cycle arrest at the G0/G1 phase (Fig. 2H). All of the above results indicated that RB cell proliferation is regulated by LSD1.

LSD1 Inhibitor SP2509 Suppresses the LSD1-Induced Increases in Y79 and Weri-RB1 Cell Proliferation In Vitro

SP2509 is a pan-HDAC inhibitor that has a potent antiproliferative effect.[21] Considering the above results, we performed MTT and colony formation assays to determine whether SP2509 inhibits RB cell proliferation. As a result, SP2509 inhibited Y79 and Weri-RB1 cell viability in a concentration- and time-dependent manner. The IC50 values of SP2509 were 1.22 μM and 0.47 μM for 48 hours and 72 hours, respectively, in Y79 cells, whereas Weri-RB1 cells with high LSD1 expression were more sensitive to SP2509 (IC50 values of 0.73 μM and 0.24 μM for 48 hours and 72 hours, respectively). At the same concentration, the ability of SP2509 to inhibit the viability of normal cells was reduced (Fig. 3A). As shown in Figure 3B, RB cells but not normal cells exhibited a significant decrease in the number of colonies after treatment with SP2509 compared with that in the control-treated

Investigative Ophthalmology & Visual Science

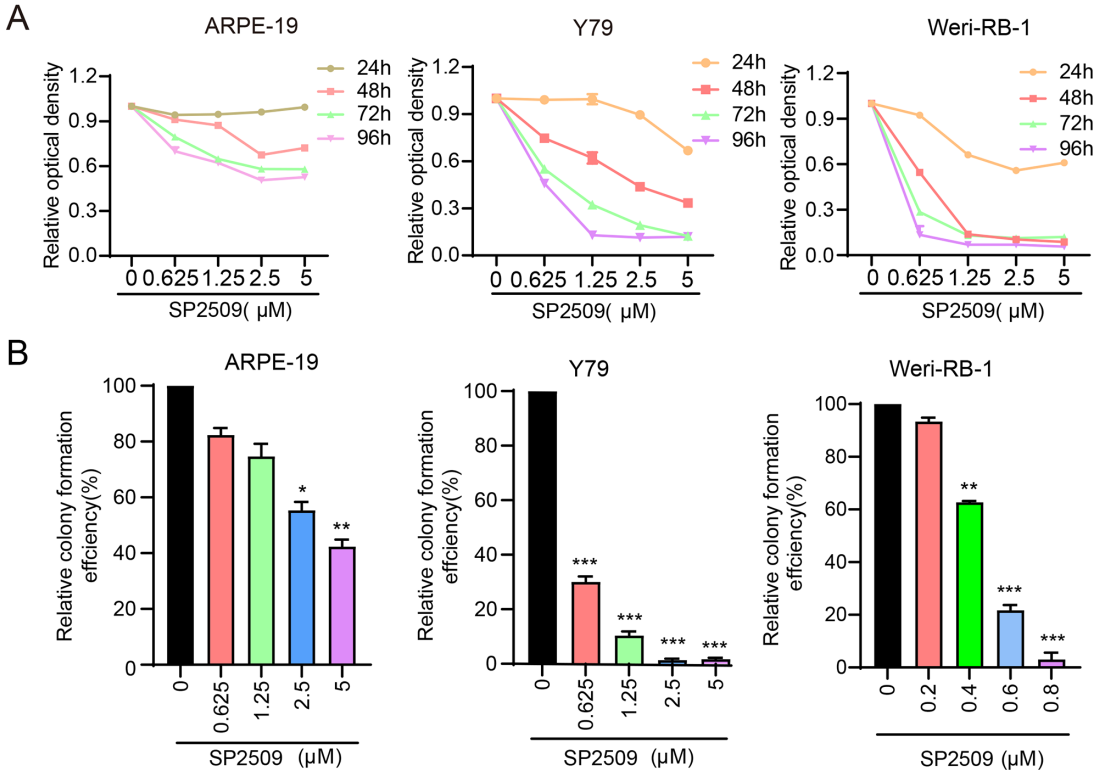

Figure 3. The LSD1 antagonist SP2509 reduces RB cell proliferation but has no significant influence on ARPE-19 under the same conditions. (**A**, **B**) Proliferation of three cell lines (Y79, Weri-RB1, and ARPE-19) treated with SP2509 was evaluated by an MTT assay and a colony formation assay. The data are reported as the means ± standard deviations ($n = 3$), Student's t-test, $^{*}P < 0.05$, $^{**}P < 0.01$, $^{***}P < 0.001$.

cells. Consistent with the above results, SP2509 suppressed LSD1-induced cell proliferation.

SP2509 Induces Cell Cycle Arrest at G0/G1 Phase and Apoptosis of Y79 and Weri-RB1 Cells

The cell cycle distribution of RB cells was detected using flow cytometry. As expected, the percentage of cells in the G0/G1 phase gradually increased as the concentration of SP2509 increased, and the percentage of cells in the S/G2 phase gradually decreased (Figs. 4A, B). Collectively, our results indicated that SP2509 induces cell cycle arrest at the G0/G1 phase. Subsequently, apoptosis assays were performed, and a higher percentage of RB cells in regions Q2 and Q3 was observed after treatment with SP2509 for 48 hours. As shown in Figures 4C, D, Y79 cells treated with 0, 2.5 μM, and 5 μM SP2509 exhibited apoptosis rates of 15.07%, 20.14%, and 31.3%, respectively, whereas the apoptosis rates in Weri-RB1 cells treated with 0, 1, and 2 μM SP2509 were 25%, 37%, and 39.64%, respectively. Western blot analyses confirmed apoptosis induction via increased levels of cleaved caspase 3 and PARP (Figs. 4E, F). Our results indicate that SP2509 inhibits LSD1-induced cell proliferation via arrest at the G1/S transition and subsequent apoptosis.

Treatment With SP2509 Induces H3K4me2 Expression and Inhibits β-catenin Signaling Pathway-Related Protein Expression in Y79 and Weri-RB1 Cells

RNA sequencing (RNA-seq) technology was used to elucidate the antiproliferative and proapoptotic mechanisms of SP2509. Transcriptome analysis results showed that 2378 genes were markedly upregulated and 669 genes were significantly downregulated (Fig. 5A), with Q values <0.001 and fold change ≥2. Among these genes, 75 genes were highly correlated with cell growth and death (Fig. 5B). RT-PCR was performed to confirm four upregulated genes, p16, p19, p21, and GADD45β, and two downregulated genes, C-myc and cyclin D3, and the results were consistent with the RNA-seq results (Fig. 5C). KEGG pathway analysis revealed that the inhibitory effect of SP2509 was associated with genes involved in the Wnt signaling pathway (Fig. 5D). Evidence from the literature states that LSD1 inhibition promotes histone methylation,[22] which we have confirmed. Western blot assays illustrated that the protein levels of β-catenin, C-myc, and cyclin D3 decreased after SP2509 treatment (Figs. 5E, F). All of the above results indicate that the antitumor mechanism of SP2509 is related to β-catenin signaling.

SP2509 Exerts Significant Inhibition of Y79 Xenograft Growth

Due to the antiproliferative effect on RB cells in vitro, we investigated the in vivo antitumor effect of SP2509 by conducting subcutaneous xenograft experiments in BALB/c nude mice. First, SP2509 (25 mg/kg/d, intraperitoneal injection) was shown to significantly suppress tumor growth without affecting the total body weight of the animals (Figs. 6A–D). We also assessed the Wnt/β-catenin signaling pathway in vivo, and the protein levels of β-catenin, c-MYC, and cyclin D3 were assayed by Western blot. The results revealed decreased levels of β-catenin, c-MYC, and cyclin D3, similar to the in vitro results (Figs. 6E, F).

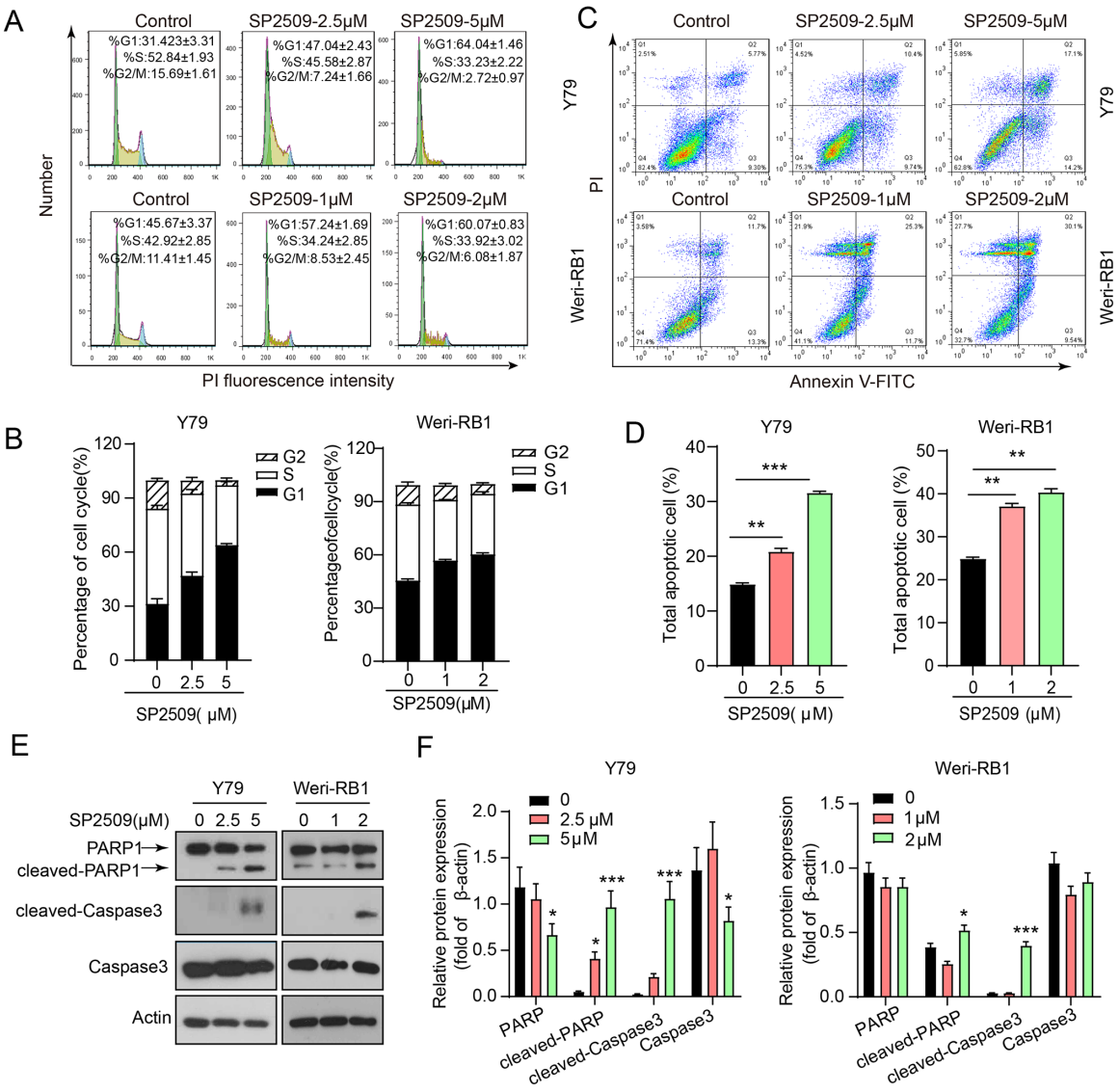

Figure 4. SP2509 induces cell cycle arrest at G0/G1 phase and apoptosis of Y79 and Weri-RB1 cells. (**A**, **B**) The cell cycle distribution was assayed by flow cytometry, and SP2509 significantly induced G0/G1 cell cycle arrest in Y79 and Weri-RB1 cells. Each colored area in **A** represents cells at different phases of the cell cycle: the *green* area represents cells in G1 phase, the *yellow* area represents cells in S phase, and the *blue* area represents cells in G2/M phase. (**B**) Statistical results of the data from **A**. (**C**, **D**) Apoptosis of cells treated with SP2509 for 48 hours was evaluated via fluorescence-activated cell sorting (FACS). The data are reported as the means ± standard deviations ($n = 3$), Student's *t*-test, $^{**}P < 0.01$, $^{***}P < 0.001$. (**E**, **F**) Western blot analysis of the levels of cleaved caspase 3 and PARP in two RB cell lines treated with SP2509. The data are reported as the means ± standard deviations ($n = 3$), Student's *t*-test, $^{*}P < 0.05$, $^{***}P < 0.001$.

Discussion

RB is the most common intraocular malignancy in children, for which enucleation is the gold standard of treatment.[23] Multimodal regimens that include chemotherapy, focal treatment (such as transpupillary thermotherapy, cryotherapy and laser photocoagulation), radiation therapy, and surgery play a vital role in salvaging the globe. Nevertheless, various side effects, such as induction of secondary tumors, recurrence, and metastasis, are indicative of treatment failure; thus, new therapy strategies are urgently needed.

LSD1 overexpression has been shown to be associated with poor prognosis in a variety of tumors, such as prostate, lung, breast, and hematologic malignancies.[24–28] However, the effects and mechanisms of action underlying the role of LSD1 in RB remain unclear. In the present study, we demonstrated for the first time that the expression levels of LSD1 were significantly upregulated in primary RB tissues and RB cells (Y79 and Weri-RB1) and confirmed that RB cell proliferation is regulated by LSD1. Therefore, abnormal expression of LSD1 may also be significantly correlated with poor prognosis in patients with RB. LSD1 has been a novel therapeutic target in a number of cancers, and its inhibitors have great potential as anticancer therapies.[29–31] We also showed that suppressing LSD1 significantly inhibited RB proliferation both in vitro and in vivo; therefore, LSD1 may also be a potential therapeutic target for RB.

The effect of LSD1 on cell cycle in RB cells was explored to obtain a better understanding of the mechanism of promoting tumor proliferation. As previously reported, LSD1

Investigative Ophthalmology & Visual Science

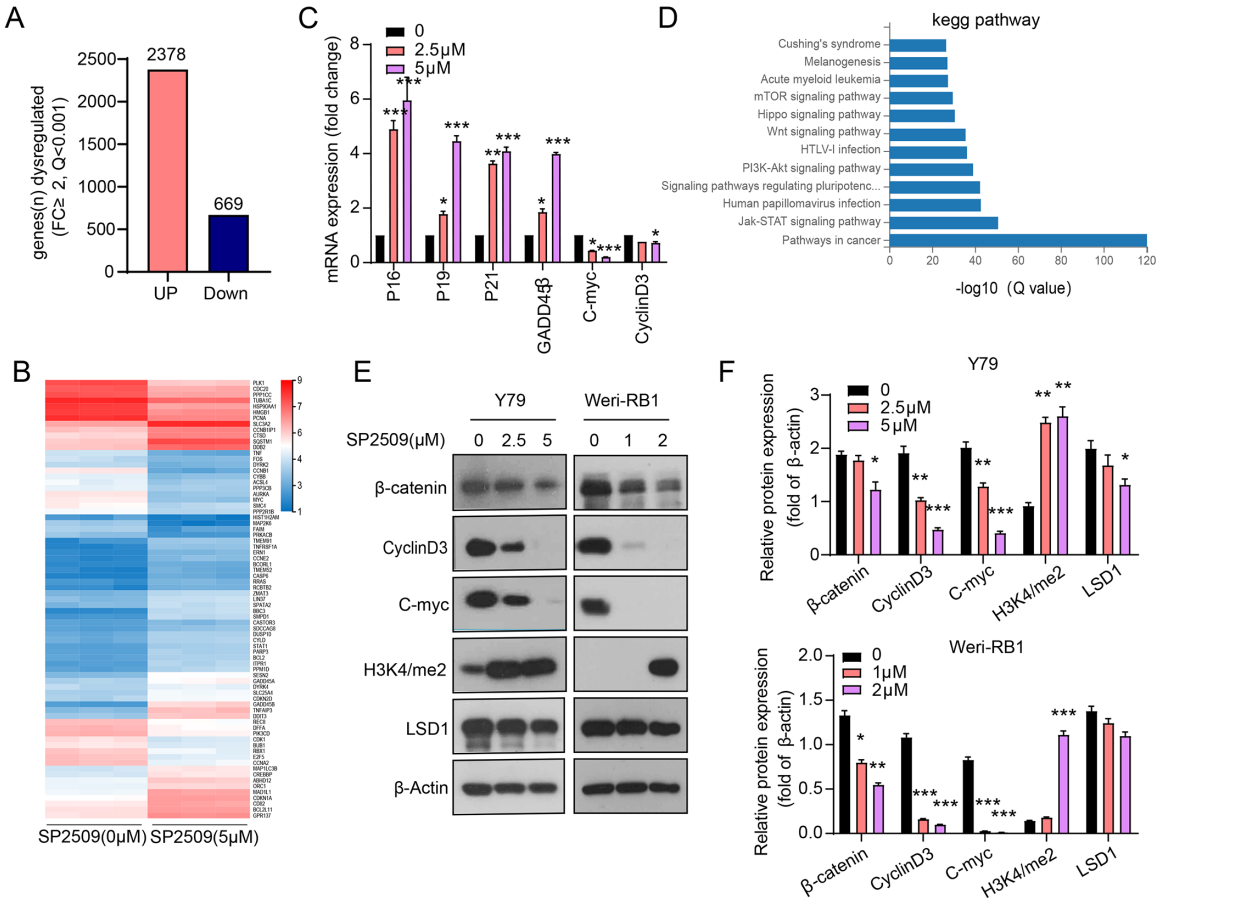

Figure 5. Treatment with SP2509 increases H3K4me2 levels and inhibits the expression of β-catenin signaling pathway–related proteins in RB cells. (**A**) RNA-seq was used to analyze the changes in mRNA expression profile of Y79 cells treated with SP2509. (**B**) Heatmap analysis of genes related to cell survival in cells treated with SP2509. (**C**) Quantitative PCR analysis of four upregulated genes (p16, p19, p21, and GADD45β) and two downregulated genes (C-myc and cyclin D3). *$P < 0.05$, **$P < 0.01$, ***$P < 0.001$. (**D**) KEGG pathway analysis of upregulated and downregulated genes. (**E**, **F**) Western blot assays were used to analyze the expression of β-catenin pathway-related proteins, LSD1, and H3K4/me2. The data are reported as the means ± standard deviations ($n = 3$), Student's t-test, *$P < 0.05$, **$P < 0.01$, ***$P < 0.001$.

binding sites overlap significantly with those bound by the S-phase gene transcription factor E2F1, promoting S-phase entry and tumorigenesis.[32] In our study, LSD overexpression weakly promoted cells from the G1 phase to the S and G2 phases, and LSD1 knockdown induced cell cycle arrest at the G0/G1 phase. The reason for weakly promoting S-phase entry may be as strongly proliferative ability and highly LSD1 expression in Y79.

The development of LSD1 inhibitors for clinical treatment of tumors is one of the most promising approaches for cancer therapy.[33] Moreover, understanding the underlying antitumor mechanisms of inhibitors is important for the effective treatment of patients. SP2509 is a novel LSD1 antagonist, and the literature states that SP2509 can significantly inhibit viability in other types of cancer cells. In our study, we demonstrated that SP2509 did not directly inhibit LSD1 expression but rather led to the accumulation of H3K4/me2 by inhibiting the activity of LSD1 in RB, which is consistent with data reported in the literature.[14] We also observed that in multiple models of RB, SP2509 exhibited potent inhibitory effects on cell proliferation and colony formation, induced G1/S phase arrest and apoptosis in vitro, and ameliorated tumor growth in vivo. This suggests that SP2509 is a potential candidate for RB treatment. Previous work has demonstrated that SP2509 targets JAK/STAT signaling in various cancer cells[34] and engages the endoplasmic reticulum stress pathway in the treatment of Ewing sarcoma.[16] In the present study, we observed that the antitumor mechanism of SP2509 is at partially mediated by suppression of the β-catenin pathway. The protein expression of P21, P16, and P19 was significantly altered in our study, but additional research of biochemical mechanisms is still necessary.

Cisplatin (DDP) is a well-known chemotherapy drug that has been widely used to treat different types of cancers, such as bladder cancer, head and neck cancer, sarcoma, and bone cancer.[35] It is also a common chemotherapeutic agent for RB.[36] Recently, chemotherapy drugs combined with other drugs to enhance their efficacy, reduce toxicity, and overcome drug resistance have gradually been introduced in the treatment of cancer.[37,38] In our study, we explored whether SP2509 and cisplatin exerted synergistic effects and whether the combination of these two drugs affects colony formation, apoptosis, and the expression of apoptosis-related proteins. No obvious synergistic effect between the two drugs was found (data not shown), but further experiments on combinations with other drugs, which may be more effective in treating RB, need to be explored.

Investigative Ophthalmology & Visual Science

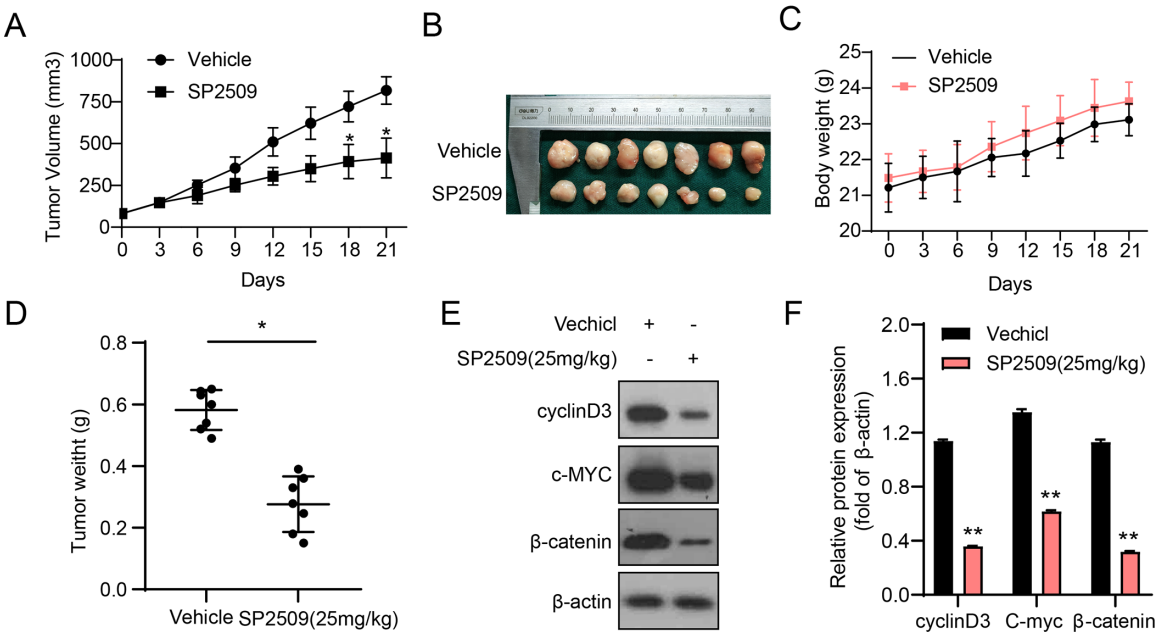

Figure 6. SP2509 inhibits Y79 xenograft tumor growth. (**A**, **B**) Tumor size and total body weight measured at the indicated time points in the two groups. (**C**, **D**) Tumor tissues were removed and weighed after 21 days of treatment. (**E**, **F**) Western blot assays were used to detect the β-catenin, C-myc, and cyclin D3 protein levels in tumor tissues after 21 days of SP2509 treatment. (**A**, **D**, **F**) Student's *t*-test, $^{*}P < 0.05$, $^{**}P < 0.01$.

In conclusion, our study highlighted an important role of LSD1 in promoting tumor growth in RB. LSD1 may serve as a valuable target for treating patients with RB and clinical translational research.

Acknowledgments

Supported by grants from the National Natural Science Foundation of China (No. 82060501 to HG), the Natural Science Foundation of Jiangxi Province (No. 20202ACB206005 to HG), and the Nanchang Science and Technology Bureau (Hong Ke Zi [2020] No. 137).

Disclosure: **A. Jiang**, None; **W. Wu**, None; **C. Xu**, None; **L. Mao**, None; **S. Ao**, None; **H. Guo**, None; **X. Sun**, None; **J. Tao**, None; **Y. Sang**, None; **G. Huang**, None

References

1. Fabian ID, Onadim Z, Karaa E, et al. The management of retinoblastoma. *Oncogene*. 2018;37(12):1551–1560.
2. Aubry A, Pearson JD, Huang K, et al. Functional genomics identifies new synergistic therapies for retinoblastoma. *Oncogene*. 2020;39(31):5338–5357.
3. Errico A. Cancer therapy: retinoblastoma—chemotherapy increases the risk of secondary cancer. *Nat Rev Clin Oncol*. 2014;11(11):623.
4. Dyer MA. Lessons from retinoblastoma: implications for cancer, development, evolution, and regenerative medicine. *Trends Mol Med*. 2016;22(10):863–876.
5. Gu F, Lin Y, Wang Z, et al. Biological roles of LSD1 beyond its demethylase activity. *Cell Mol Life Sci*. 2020;77:3341–350.
6. Shi Y, Lan F, Matson C, et al. Histone demethylation mediated by the nuclear amine oxidase homolog LSD1. *Cell*. 2004;119(7):941–953.
7. Kim SA, Zhu J, Yennawar N, Eek P, Tan S, et al. Crystal structure of the LSD1/CoREST histone demethylase bound to its nucleosome substrate. *Mol Cell*. 2020;78(5):903–914.e4.
8. Maes T, Mascaró C, Tirapu I, et al. ORY-1001, a potent and selective covalent KDM1A inhibitor, for the treatment of acute leukemia. *Cancer Cell*. 2018;33(3):495–511.e12.
9. Park DE, Cheng J, McGrath JP, et al. Merkel cell polyomavirus activates LSD1-mediated blockade of non-canonical BAF to regulate transformation and tumorigenesis. *Nat Cell Biol*. 2020;22(5):603–615.
10. Sehrawat A, Gao L, Wang Y, et al. LSD1 activates a lethal prostate cancer gene network independently of its demethylase function. *Proc Natl Acad Sci USA*. 2018;115(18):E4179–E4188.
11. Macheleidt IF, Dalvi PS, Lim SY, et al. Preclinical studies reveal that LSD1 inhibition results in tumor growth arrest in lung adenocarcinoma independently of driver mutations. *Mol Oncol*. 2018;12(11):1965–1979.
12. Hu X, Xiang D, Xie Y, et al. LSD1 suppresses invasion, migration and metastasis of luminal breast cancer cells via activation of GATA3 and repression of TRIM37 expression. *Oncogene*. 2019;38(44):7017–7034.
13. Mohammad HP, Smitheman KN, Kamat CD, et al. A DNA hypomethylation signature predicts antitumor activity of LSD1 inhibitors in SCLC. *Cancer Cell*. 2015;28(1):57–69.
14. Fiskus W, Sharma S, Shah B, et al. Highly effective combination of LSD1 (KDM1A) antagonist and pan-histone deacetylase inhibitor against human AML cells. *Leukemia*. 2014;28(11):2155–2164.
15. Zhu L, Hu L, Liu L, et al. LSD1 inhibition suppresses the growth of clear cell renal cell carcinoma via upregulating P21 signaling. *Acta Pharm Sin B*. 2019;9(2):324–334.
16. Pishas KI, Drenberg CD, Taslim C, et al. Therapeutic targeting of KDM1A/LSD1 in Ewing sarcoma with SP-2509 engages the endoplasmic reticulum stress response. *Mol Cancer Ther*. 2018;17(9):1902–1916.
17. Liu X, He J, Mao L, et al. EPZ015666, a selective protein arginine methyltransferase 5 (PRMT5) inhibitor with an antitumour effect in retinoblastoma. *Exp Eye Res*. 2021;202:108286.

18. Chévez-Barrios P, Hurwitz MY, Louie K, et al. Metastatic and nonmetastatic models of retinoblastoma. *Am J Pathol*. 2000;157(4):1405–1412.
19. Zhang Y, Duan S, Jang A, Mao L, Liu X, Huang G. JQ1, a selective inhibitor of BRD4, suppresses retinoblastoma cell growth by inducing cell cycle arrest and apoptosis. *Exp Eye Res*. 2020;202:108304.
20. Hosseini A, Minucci S. A comprehensive review of lysine-specific demethylase 1 and its roles in cancer. *Epigenomics*. 2017;9(8):1123–1142.
21. Fiskus W, Sharma S, Shah B, et al. Highly effective combination of LSD1 (KDM1A) antagonist and pan-histone deacetylase inhibitor against human AML cells. *Leukemia*. 2017;31(7):1658.
22. Wu B, Pan X, Chen X, et al. Epigenetic drug library screening identified an LSD1 inhibitor to target UTX-deficient cells for differentiation therapy. *Signal Transduct Target Ther*. 2019;4:11.
23. Abramson DH, Gobin YP, Francis JH. Orbital retinoblastoma treated with intra-arterial chemotherapy. *Ophthalmology*. 2021;128(10):1437.
24. Lv T, Nie FQ, Wang Q, et al. Over-expression of LSD1 promotes proliferation, migration and invasion in non-small cell lung cancer. *PLoS One*. 2012;7(4):e35065.
25. Wang Y, Zhu Y, Wang Q, et al. The histone demethylase LSD1 is a novel oncogene and therapeutic target in oral cancer. *Cancer Lett*. 2016;374(1):12–21.
26. Liu J, Feng J, Li L, et al. Arginine methylation-dependent LSD1 stability promotes invasion and metastasis of breast cancer. *EMBO Rep*. 2020;21(2):e48597.
27. Augert A, Eastwood E, Ibrahim AH, et al. Targeting NOTCH activation in small cell lung cancer through LSD1 inhibition. *Sci Signal*. 2019;12(567):eaau2922.
28. Lee C, Rudneva VA, Erkek S, et al. Lsd1 as a therapeutic target in Gfi1-activated medulloblastoma. *Nat Commun*. 2019;10(1):332.
29. Li Y, Tao L, Zuo Z, et al. ZY0511, a novel, potent and selective LSD1 inhibitor, exhibits anticancer activity against solid tumors via the DDIT4/mTOR pathway. *Cancer Lett*. 2019;454:179–190.
30. Leiendecker L, Jung PS, Krecioch I, et al. LSD1 inhibition induces differentiation and cell death in Merkel cell carcinoma. *EMBO Mol Med*. 2020;12(11):e12525.
31. Salamero O, Montesinos P, Willekens C, et al. First-in-human phase I study of iadademstat (ORY-1001): a first-in-class lysine-specific histone demethylase 1A inhibitor, in relapsed or refractory acute myeloid leukemia. *J Clin Oncol*. 2020;38(36):4260–4273.
32. He Y, Zhao Y, Wang L, et al. LSD1 promotes S-phase entry and tumorigenesis via chromatin co-occupation with E2F1 and selective H3K9 demethylation. *Oncogene*. 2018;37(4):534–543.
33. Fang Y, Yang C, Teng D, et al. Natural products as LSD1 inhibitors for cancer therapy. *Acta Pharm Sin B*. 2021;11(3):621–631.
34. Zhen H, Zhang X, Zhang L, et al. SP2509, an inhibitor of LSD1, exerts potential antitumor effects by targeting the JAK/STAT3 signaling. *Acta Biochim Biophys Sin (Shanghai)*. 2021;53(8):1098–1105.
35. Dasari S, Tchounwou PB. Cisplatin in cancer therapy: molecular mechanisms of action. *Eur J Pharmacol*. 2014;740:364–378.
36. Song HB, Jun HO, Kim JH, et al. Anti-apoptotic effect of clusterin on cisplatin-induced cell death of retinoblastoma cells. *Oncol Rep*. 2013;30(6):2713–2718.
37. Kanai M, Hatano E, Kobayashi S, et al. A multi-institution phase II study of gemcitabine/cisplatin/S-1 (GCS) combination chemotherapy for patients with advanced biliary tract cancer (KHBO 1002). *Cancer Chemother Pharmacol*. 2015;75(2):293–300.
38. Sun F, Zhang Y, Xu L, et al. Proteasome inhibitor MG132 enhances cisplatin-induced apoptosis in osteosarcoma cells and inhibits tumor growth. *Oncol Res*. 2018;26(4):655–664.

Investigative Ophthalmology & Visual Science